

# Systematic reduction of magnetization by an ac transverse field and of the anomalous magnetization peak in a N<sub>2</sub>-annealed Tl<sub>2</sub>Ba<sub>2</sub>CuO<sub>6</sub> single crystal

Dong Ho Kim\*

*Department of Physics and Institute of Optics and Nano-Technology, Yeungnam University, Gyeongsan 712-749, Korea*

Heon-Jung Kim, N. H. Dan, and Sung-Ik Lee

*National Creative Research Initiative Center for Superconductivity and Department of Physics,**Pohang University of Science and Technology, Pohang 790-784, Korea*

(Received 2 February 2004; revised manuscript received 18 May 2004; published 30 December 2004)

Measurements of magnetization of N<sub>2</sub>-annealed Tl<sub>2</sub>Ba<sub>2</sub>CuO<sub>6</sub> were carried out by using a micro-Hall sensor while applying a low-ac transverse magnetic field  $H_{ac}$  along the  $ab$  plane in addition to a dc magnetic field along the  $c$  axis. A systematic reduction of dc magnetization was observed, and further, an anomalous second magnetization peak evolved with increasing  $H_{ac}$ . We explained the observed reduction of magnetization due to a dc electric field generated by an ac transverse field, which leads to the decay of the magnetization and then interpreted the development of the second peak at finite  $H_{ac}$  due to the destruction of the vortex lattice by strong point pinning and the subsequent optimal redistribution of two-dimensional vortices to the pinning centers.

DOI: 10.1103/PhysRevB.70.214527

PACS number(s): 74.25.Ha, 74.25.Qt

## I. INTRODUCTION

Vortex properties of high-temperature superconductors have been extensively studied by transport and magnetization. One efficient method to investigate the vortex matter is measuring magnetization while dithering vortices by applying a small ac transverse magnetic field. When an in-plane ac magnetic field is superposed with the dc magnetic field along the crystalline  $c$  axis, the vortices will experience time-varying torque by an ac field. This vortex dithering causes effective reduction of pinning energy, which, in turn, gives rise to a reduction of irreversible magnetization. Recently, this experimental approach has been used to study the shift of the irreversibility line in YBa<sub>2</sub>Cu<sub>3</sub>O<sub>7- $\delta$</sub>  (YBCO) (Ref. 1) and the nature of the second magnetization peak in Bi<sub>2</sub>Sr<sub>2</sub>CaCu<sub>2</sub>O<sub>8</sub> (Bi-2212), in which an order of tens of gauss of an ac transverse magnetic field significantly reduced the magnetization.<sup>2,3</sup> Suppression of the magnetic moment has been also observed in a different geometry where a dc field is parallel to the  $ab$  plane.<sup>4,5</sup> Theoretically, the magnetic behavior of thin superconductors by a small ac transverse field has been treated by Brandt and Mikitik<sup>6</sup> and Mikitik and Brandt.<sup>7</sup> The ac field periodically tilts the vortex in the critical state, where magnetic induction is nonuniform. The tilt is not symmetric relative to the center of the sample, and this asymmetry leads to a shift of vortices toward the relaxed state during each cycle. Thus the reduction of irreversible magnetization is due to the cyclic distortion of the flux lines, which macroscopically walk toward the relaxed state.

Tl<sub>2</sub>Ba<sub>2</sub>CuO<sub>6</sub> (Tl-2201) lies between YBCO and Bi-2212 in terms of anisotropy. Low-field magnetization studies showed the different behavior in two different orientations of field parallel to the  $c$  axis and  $ab$  plane, while in less anisotropic YBCO, similar behavior was observed for both field orientations.<sup>8</sup> These results revealed that Tl-2201 is in the same class of Bi-2212 as the dimensionality is concerned,

although the penetration depth anisotropy is around 25 compared to 250 of Bi-2212.<sup>8</sup> Therefore, it is of interest to study how an ac transverse magnetic field suppresses the magnetic moment in less anisotropic Tl-2201 and to compare with earlier results on Bi-2212 and YBCO.<sup>1,2</sup> In this work we analyzed the effects of an ac transverse magnetic field  $H_{ac}$  on the irreversible magnetization of an N<sub>2</sub>-annealed Tl-2201 single crystal as a function of ac field and temperature. A second anomalous magnetization peak was not observed with  $H_{ac}=0$  in this N<sub>2</sub>-annealed sample, which, on the other hand, has been observed in previously studied Tl<sub>2</sub>Ba<sub>2</sub>CuO<sub>6</sub>,<sup>9-11</sup> similar to Tl<sub>2</sub>Ba<sub>2</sub>CaCu<sub>2</sub>O<sub>8</sub>,<sup>12</sup> Bi<sub>2</sub>Sr<sub>2</sub>CaCu<sub>2</sub>O<sub>8</sub>,<sup>2,3,13</sup> and other materials.<sup>14,15</sup> However, the anomalous magnetization peak evolved with increasing  $H_{ac}$ , especially at high temperatures within our experimental window. We first explain the observed reduction of magnetization by  $H_{ac}$  using the model proposed by Brandt and Mikitik,<sup>6</sup> and interpret the development of the second peak at finite  $H_{ac}$  due to the destruction of the vortex lattice by strong pinning followed by optimal redistribution of two-dimensional (2D) vortices to the pinning centers.<sup>16</sup>

## II. EXPERIMENTS

Single crystals of Tl<sub>2</sub>Ba<sub>2</sub>CuO (Tl-2201) were grown by a self-flux method, following a two-step method. In the first step, a 10 g polycrystalline pellet of Tl-2201 was made from a stoichiometric mixture of Tl<sub>2</sub>O<sub>3</sub>, BaO, and CuO and was fired at 850 °C for 15 min in a preheated furnace. Then, the pellet was reground and was mixed with additional 10% CuO and 15% Tl<sub>2</sub>O<sub>3</sub> by weight. The additional CuO was used as a flux and Tl<sub>2</sub>O<sub>3</sub> compensated for the loss of Tl during the crystal growth. The mixture was again pressed into a pellet and put into the preheated furnace at 930 °C. The crystal growth was performed inside a tightly covered crucible to minimize the loss of Tl. The temperature was

lowered to 870 °C for 15 hr. Samples were later post annealed at 400 °C in N<sub>2</sub> environment for 24 hr and slowly cooled to room temperature just before taking measurements. Crystal dimension was  $1.2 \times 1.3 \times 0.05$  mm<sup>3</sup>.

The transition temperatures  $T_c$  was 83 K as determined from the zero-field-cooled and field-cooled magnetization in a magnetic field of 10 G applied parallel to the  $c$  axis. An InSb Hall sensor of sensing area  $100 \times 100$  μm<sup>2</sup> was used to measure the local magnetic field. The TI-2201 crystal was mounted on the center of the Hall sensor unit and then inserted into a Cu-wire wound small solenoid such that the solenoid axis is perpendicular to the  $c$  axis. In this geometry the ac magnetic field was in the  $ab$  plane and dc field along the  $c$  axis of crystal. Magnetization loops were measured over a temperature range of  $20 \text{ K} < T < 80 \text{ K}$  with varying  $H_{ac}$  and its frequency. Details of the experimental conditions were described elsewhere.<sup>3</sup> The magnitude of  $H_{ac}$  was varied up to 28.8 G, and the frequency of ac field was 101 Hz.

### III. RESULTS AND DISCUSSION

The Hall sensor measures the component of local magnetic induction parallel to the crystalline  $c$  axis  $B_z$ , then  $B_z - \mu_0 H$ , where  $H$  is the dc magnetic field, is proportional to the sample magnetization. Comparing this method to the global magnetization measurement by a superconducting quantum interference device (SQUID) magnetometer showed a good agreement between two different methods.<sup>12</sup> For convenience, we will use the word “magnetization” in the text in place of  $B_z - \mu_0 H$ , even though the measured data are merely proportional to the real magnetization.

Figure 1 shows effects of  $H_{ac}$  on the magnetization at 40 K (a) and 70 K (b). The systematic reduction of magnetization with increasing  $H_{ac}$  is clearly observable, and the relative reduction under the same  $H_{ac}$  is much higher at 70 K. At 70 K, an additional peak feature developed with increasing  $H_{ac}$ , which was absent at  $H_{ac}=0$ . Within our  $H_{ac}$  range, such a peak feature was observed only above 60 K.

In order to compensate the temperature effect on the systematic reduction of irreversible magnetization  $\Delta M$ , due to  $H_{ac}$ , we normalized  $\Delta M$  by  $\Delta M$  at  $H_{ac}=0$  [i.e.,  $\Delta M(H_{ac}, T)/\Delta M(0, T)$ ]. Figure 2 shows a summary of  $\Delta M_0(H_{ac}, T)/\Delta M_0(0, T)$  at  $H=0$  (remnant magnetization) as a function of  $H_{ac}$  at various temperatures. The  $\Delta M_H(H_{ac}, T)/\Delta M_H(0, T)$  at  $H \neq 0$  exhibited qualitatively similar dependence on  $H_{ac}$  as will be shown in Fig. 3(a). The relative reduction of the magnetization becomes larger with increasing temperature and  $H_{ac}$  due to lowering of the effective pinning energy. At low  $H_{ac}$ , the normalized magnetization first slowly decreases, but after a threshold field of  $H_{ac}$ ,  $\Delta M$  decreases monotonically within our ac field range. At low-enough temperatures, a field of  $H_{ac}=4.8$  G was not high enough to provoke any noticeable suppression of  $\Delta M$ .

To understand the systematic behavior of  $\Delta M$  as a function of  $T$  and  $H_{ac}$ , we adapted a model developed by Brandt and Mikitik.<sup>6</sup> When a thin-strip superconductor is placed in a dc magnetic field normal to the strip, applying a weak ac in-plane field leads to a generation of a dc voltage along the strip line. This dc voltage may be interpreted as generated by

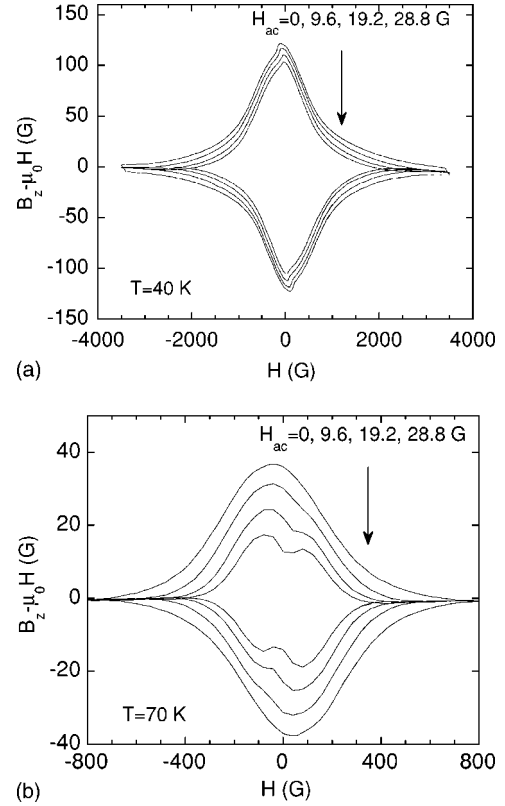


FIG. 1. A systematic reduction of magnetization measured at 40 K (a) and 70 K (b) with an increasing ac transverse magnetic field  $H_{ac}$  is shown. The relative reduction under the same  $H_{ac}$  was much higher at 70 K, and an additional peak evolved with increasing  $H_{ac}$ .

transfer of the flux in the direction perpendicular to the strip direction. In the critical state during the dc field sweep up, the vortices “walk” toward the center of the strip and vice versa during the field sweep down. Because of this slow walking, the sheet current  $J$  tends to relax with exponentially in time after some transient time as

$$J(t) = CJ_c(0)\exp(-t/\tau), \quad (1)$$

where  $C$  is a constant depending on the magnetic history, and  $J_c(0)$  is the critical current when  $H_{ac}$  is switched on. The relaxation time  $\tau$  is given by

$$\tau^{-1} = Af \frac{H_{ac} - H_p}{J_c(0)}, \quad (2)$$

where  $f$  is the frequency of the ac field and  $A$  is a constant depending on the ratio of the thickness  $d$  to the width  $w$  of the the strip, and in this case,  $A \approx 16d/w \approx 0.6$  using the numerical value in Ref. 5. Equation (2) is valid when  $H_{ac}$  fully penetrates the slab and  $H_p$  is the field of full penetration. For a infinite strip of thickness  $d$  with isotropic critical current density  $j_c$ ,  $H_p$  is given as  $H_p = j_c d/2$ . However, for the layered superconductors, such as our sample or Bi-2212, the anisotropy of the critical current should be considered. While  $J_c$  in the denominator of Eq. (2) flows in the plane to give rise to the magnetic moment,  $j_c$  associated with  $H_p$  con-

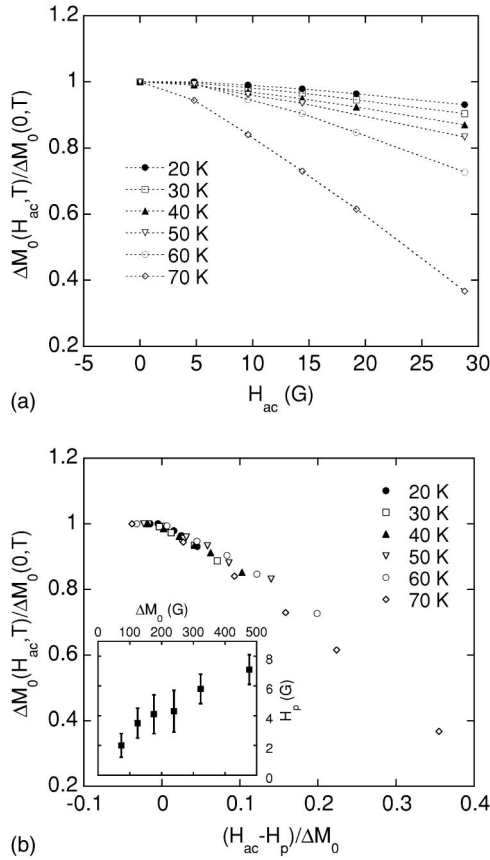


FIG. 2. (a) Relative reduction of the normalized remnant magnetization as a function of  $H_{ac}$  at various temperatures. With increasing temperature, the relative reduction increases systematically. Lines are a guide to the eye. (b) Scaling of remnant magnetization as a function of  $(H_{ac} - H_p)/\Delta M_0(0, T)$ . The inset shows full penetration fields  $H_p$  with error bars used for the plot as a function of  $\Delta M_0(0, T)$ .

sists of contributions from both in-plane and out-of-plane current component considering the ac-field penetration into the sample.<sup>17</sup> Since the magnetic field penetration from the side is much easier than the penetration from the flat surface, the penetration field is determined by the product of the  $c$ -axis critical current density  $j_{c\perp}$  and the width of the sample, as have been verified for Bi-2212 single crystals of the similar shape to our crystals.<sup>17</sup> Then  $H_p = j_{c\perp} w/2$  for the present geometry.

In just a few cycles of  $H_{ac}$  after  $H_{ac}$  is switched on, the magnetic moment decays exponentially to the equilibrium value as observed in YBCO in accordance with Eq. (1).<sup>1,4</sup> In our experiment,  $H_{ac}$  was turned on all the time throughout the field sweep and measurement procedure, thus all the shaken, weakly pinned vortices had already been washed out by  $H_{ac}$  when we took the first local field measurement, which is about 5 s after the dc magnetic field settling. Hence, what we measured is the local magnetic field at the center of the sample in the just formed critical state consisted of the unshaken, strongly pinned vortices. The magnetic relaxation measurement with continuous  $H_{ac}$  exhibited the logarithmic time dependence, different from the exponential time dependence in Eq. (1). This result supports that we are in the new

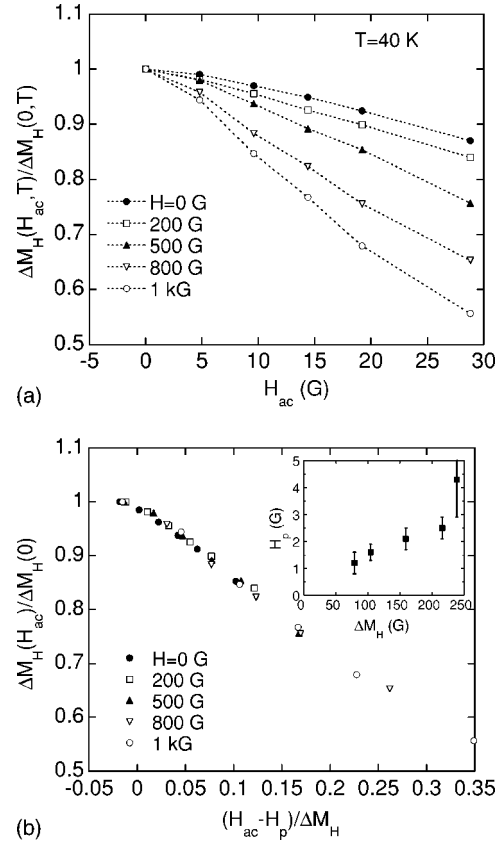


FIG. 3. (a) Relative reduction of normalized magnetization at various dc magnetic fields as a function of  $H_{ac}$  measured at 40 K. Overall behaviors are quite similar to Fig. 2(a), except the role of temperature has been replaced by a dc field. (b) A plot of magnetization as a function of  $(H_{ac} - H_p)/\Delta M_H(0, T)$ . The inset shows threshold fields  $H_p$  used for the plot as a function of  $\Delta M_H(0, T)$ .

critical state. With increasing  $H_{ac}$ , only strongly enough pinned vortices will survive and the irreversible magnetization decreases accordingly. In this case, the relaxation equation of Eq. (1) is not directly applicable to describe our results because the theory does not account for the pinning effect. However, the relaxation rate given in Eq. (2) can be a measure of the pinning strength because the rate is inversely proportional to the critical current, a quantity proportional to the pinning potential in the first order. Therefore, analyzing the systematic suppression of the magnetization by  $H_{ac}$  in terms of the  $(H_{ac} - H_p)/J_c(0)$  would be a useful exercise. In order to apply this concept to the experiment data, we replaced  $J_c(0)$  by  $\Delta M_0(0, T)$  because the decay occurred during the first 5 s when  $H_{ac} = 0$  can be safely neglected when compared to the much faster decay in the presence of  $H_{ac}$ .

Figure 2(b) is the plot of  $\Delta M_0(H_{ac}, T)/\Delta M_0(0, T)$  versus  $(H_{ac} - H_p)/\Delta M_0(0, T)$  from 20 to 70 K with  $H_p$  determined from the onset of the decreasing part of  $\Delta M_0(H_{ac}, T)/\Delta M_0(0, T)$ . One can see a collapse of the data of different temperatures on a single curve, which agrees well with our assumption that  $\tau^{-1}$  is a good indicator for the fraction of shaken vortices, and this agreement further suggests that the decrease of the magnetic moment is due to the generation of the dc electric field by the ac magnetic field applied normal

to the main dc field.<sup>6</sup> If we put the scaling behavior of Fig. 2(b) in the form of equation, it can be written as

$$\frac{\Delta M_0(H_{ac}, T)}{\Delta M_0(0, T)} \sim F\left(\frac{H_{ac} - H_p}{\Delta M_0(0, T)}\right), \quad (3)$$

where  $F$  is a scaling function. The inset of Fig. 2(b) shows the resulted  $H_p$  versus  $\Delta M_0(0, T)$ . The errors occurred while taking the onset values of  $H_{ac}$ , shown as error bars. The values at the symbols were used to plot the main panel of Fig. 2(b). The rough proportionality between  $H_p$  and  $\Delta M_0(0, T)$  is expected from the relation that  $H_p = j_{c\perp} w / 2$  and  $j_{c\perp} \propto J_c$ . If we put  $H_p \sim 7$  G for 20 K,  $j_{c\perp} \sim 1 \times 10^2$  A/cm<sup>2</sup>, which is similar to the results of Bi-2212 at 25 K (Ref. 17).

The scaling behavior of magnetization at  $H=0$  can be extended to the finite dc field case. The  $H_{ac}$  dependence of irreversible magnetization at finite  $H$ ,  $\Delta M_H$ , is summarized in Fig. 3(a), for example, for 40 K. The role of temperature in Fig. 2(a) has been replaced by the dc magnetic field. A systematic reduction of  $\Delta M_H$  with an increasing dc field can be understood by replacing the zero-field magnetization in Eq. (3) with the finite-field magnetization

$$\frac{\Delta M_H(H_{ac}, T)}{\Delta M_H(0, T)} \sim F\left(\frac{H_{ac} - H_p}{\Delta M_H(0, T)}\right). \quad (4)$$

Figure 3(b) shows a universal behavior of  $\Delta M_H(H_{ac}, T) / \Delta M_H(0, T)$ , given by Eq. (4). A good collapse of curves from different dc fields to a single curve was observed similar to Fig. 2(b). The inset shows  $H_p$  versus  $\Delta M_H(0, T)$ , and they also exhibit a rough proportionality. If we combine both data of Figs. 2(b) and 3(b) into a single plot, they fall onto a single curve showing that Eq. (4) is an applicable scaling relation regardless of temperature or a dc magnetic field. Again the relatively good agreement of the data with Eq. (4) supports that the walking flux-line model is useful to understand the effect of an ac transverse magnetic field on the suppression of the magnetization.

As mentioned earlier, a dip (or peak) in the magnetization loop evolved as  $H_{ac}$  is increased at high temperatures, as shown in Fig. 1(b). The dip started to appear at different  $H_{ac}$ , depending on the temperature, and the onset ac fields were roughly 4.8, 9.6, and 28.8 G at 80, 70, and 60 K, respectively. The peak position was also dependent on the temperature and  $H_{ac}$ . The peak effect, or fishtail feature, has already been observed in oxygen-overdoped Tl-2201<sup>11</sup> and the phenomena were interpreted as a possible dimensional crossover from 3D to 2D vortex structure<sup>10</sup> or an intrinsic pinning mechanism independent of oxygen defect concentrations.<sup>11</sup> If we compare the peak fields to the results of Tl-2201 of a similar  $T_c$  by Xu *et al.*,<sup>11</sup> they are in fairly good agreement, suggesting that the dip feature is reminiscent of the peak effect. Our crystals were annealed in N<sub>2</sub>, so the oxygen content would be different from those of previous works, and it may tell why no peak effect was observed in a zero ac field. For Bi-2212, the second magnetization peak was attributed to many phenomena. Among them, the nature of the second peak was intensively considered as a disorder-driven vortex solid-solid first-order transition.<sup>2</sup> But understanding such a broad peak in Fig. 1(b) in terms of the first-order phase tran-

sition is somewhat questionable. On the other hand, the matching of 2D vortices with the microstructural defects, where the dimensional crossover of the vortex structure with increasing dc field is *a priori* condition,<sup>18</sup> has been used to explain the increase of the peak after oxygen annealing and the absence of the peak after vacuum annealing.<sup>19</sup> The basic idea was that in the formation of a 3D structure, vortices may not fully utilize the existing defect configurations and the peak occurs as a result of destruction of the 3D vortex lattice while increasing the pinning effect by transforming to 2D vortices.

However, just a simple extension of this case may not be readily applied to the less anisotropic Tl-2201, where the 3D to 2D crossover field is up in the tesla region. Instead a pinning-induced transition to disordered vortex phases can be a candidate for the occurrence of the second peak in the presence of  $H_{ac}$ . The destruction of the vortex lattice by random-point pinning has been considered as a mechanism of the second peak in layered superconductors by Koshelev and Vinokur.<sup>16</sup> For Tl-2201, *ab*-plane penetration depth  $\lambda_{ab}$ , is 80 nm and the interlayer spacing  $s$  is 1.15 nm (Ref. 8). Since  $\lambda_{ab}/s$  ( $\approx 70$ ) is larger than the anisotropy  $\gamma$  of 25, Tl-2201 belongs to the case of a not-too-weak Josephson coupling. There are three different field regimes in this case.<sup>16</sup> At fields lower than a typical field  $B_{J-M} = 2\Phi_0 / (\lambda_{ab}\pi)^2 \ln[0.1\gamma^2 / \ln(\lambda_{ab}/r_w)]$ , the magnetic coupling between 2D pancake vortices dominates and above  $B_{J-M}$ , the Josephson coupling dominates, and the crossover from 3D to the quasi-2D regime takes place at the field  $B_{Jcr} \sim 4\Phi_0 / (\gamma s)^2$ , where  $\Phi_0$  is the flux quantum and  $r_w$  is the wandering distance of pancake to explore the local minima of the random potential. If we set  $\lambda_{ab} = 140$  nm at 70 K and  $r_w = 0.1\gamma s$ , the  $B_{J-M} \approx 600$  G, which is higher than the experimental peak field of 100 G at 70 K. The 3D to 2D crossover field  $B_{Jcr}$  for Tl-2201 is of the order of tesla, much higher than the Bi-2212 case due to smaller anisotropy. From this estimation, the peak is in the 3D magnetic regime, although the Josephson coupling is not too weak. Thus Tl-2201 is in a category of the intermediate region where the Josephson coupling dominates at small scales and the magnetic coupling dominates at the interaction length scale. In this region, the destruction of the Bragg glass phase by strong pinning occurs at the field  $B_x$

$$B_x \approx \frac{\Phi_0}{\lambda_{ab}^2} \left(\frac{\lambda_{ab}}{\gamma s}\right)^{3/4} \frac{T_m^{2D}}{U_p}, \quad (5)$$

where  $T_m^{2D}$  is the melting temperature of for a single pin-free 2D layer and  $U_p$  is the pinning energy.<sup>16</sup> In the presence of an ac field, the effect of all the shaken, weakly pinned vortices is removed and only the strongly enough pinned vortices contribute to the irreversible magnetization. Thus the magnetic loops measured with high-enough  $H_{ac}$  correspond to the case of strong pinning where  $U_p > T_m^{2D}$ ; that is, pinning is strong enough to destroy the 2D lattice in a single layer. If  $U_p$  is sufficiently larger than  $T_m^{2D}$ , then  $B_x$  can be around the peak field 100 G. At the peak, the the vortex lines are destroyed and the magnetization sharply increases as a result of each pancake choosing the optimum location to form an

entangled solid phase above the peak. Koshelev and Vinokur<sup>16</sup> suggested that the entangled solid above the peak would be a glassy phase, different from the quasiordered Bragg glass below the peak.

#### IV. SUMMARY

We studied the role of an ac transverse magnetic field on the magnetization of  $Tl_2Ba_2CuO_6$  single crystal. A systematic reduction of magnetization was observed with increasing  $H_{ac}$ , which was understood in the framework of the critical state theory, where the reduction is due to the generation of a

dc electric field by  $H_{ac}$ . At high-enough temperatures a second peak evolved at finite  $H_{ac}$ , and this sharp increase of the magnetization was interpreted as that for strong pinning; the vortex lattice is destroyed at the peak field and each 2D pancake vortex chooses the best pinning center by forming the entangled glass phase above the peak.

#### ACKNOWLEDGMENT

This work was supported by the Korea Science and Engineering Foundation through the Grant No. 1999-2-114-005-5.

\*Email address: dhkim@yumail.ac.kr

- <sup>1</sup>M. Willemin, C. Rossel, J. Hofer, H. Keller, A. Erb, and E. Walker, *Phys. Rev. B* **58**, R5940 (1998).  
<sup>2</sup>N. Avraham, B. Khaykovich, Y. Myasoedov, M. Rappaport, H. Shtrikman, S. E. Deldman, T. Tamegai, P. H. Kes, M. Li, M. Konczykowski, K. van der Beek, and E. Zeldov, *Nature (London)* **411**, 451 (2001).  
<sup>3</sup>D. H. Kim and T. W. Lee, *Physica C* **385**, 477 (2003).  
<sup>4</sup>L. M. Fisher, A. V. Kalinov, S. E. Savel'ev, I. F. Voloshin, V. A. Yampol'skii, M. A. R. LeBlanc, S. Hirscher, *Physica C* **278**, 169 (1997).  
<sup>5</sup>L. M. Fisher, K. V. Il'enko, A. V. Kalinov, M. A. R. LeBlanc, F. Pérez-Rodríguez, S. E. Savel'ev, I. F. Voloshin, and V. A. Yampol'skii, *Phys. Rev. B* **61**, 15 382 (2000).  
<sup>6</sup>E. H. Brandt and G. P. Mikitik, *J. Low Temp. Phys.* **131**, 1033 (2003).  
<sup>7</sup>G. P. Mikitik and E. H. Brandt, *Phys. Rev. B* **69**, 134521 (2004).  
<sup>8</sup>N. E. Hussey, J. R. Cooper, R. A. Doyle, C. T. Lin, W. Y. Liang, D. C. Sinclair, G. Balakrishnan, D. McK. Paul, and A. Revcolevschi, *Phys. Rev. B* **53**, 6752 (1996).  
<sup>9</sup>V. N. Kopylov, A. E. Koshelev, I. F. Schegolev, and T. G. Togonidze, *Physica C* **223**, 291 (1990).

- <sup>10</sup>F. Zuo, S. Khizroev, G. C. Alexandrakis, and V. N. Kopylov, *Phys. Rev. B* **52**, R755 (1995).  
<sup>11</sup>M. Xu, T. W. Li, D. G. Hinks, G. W. Crabtree, H. M. Jaeger, and H. Aoki, *Phys. Rev. B* **59**, 13 632 (1999).  
<sup>12</sup>P. Chowdhury, H.-J. Kim, W. N. Kang, D.-J. Zang, S.-Ik Lee, and D. H. Kim, *Phys. Rev. B* **68**, 134413 (2003).  
<sup>13</sup>N. Chikumoto, M. Konczykowski, N. Motohira, and A. P. Malozemoff, *Phys. Rev. Lett.* **69**, 1260 (1992).  
<sup>14</sup>M. Daeumling, J. M. Seuntjens, and D. C. Labalestier, *Nature (London)* **346**, 332 (1990).  
<sup>15</sup>Y. Abulafia, A. Shaulov, Y. Wolfus, R. Prozorov, L. Burlachkov, Y. Yeshurun, D. Majer, X. Zeldov, H. Wühl, V. B. Geshkenbein, and V. M. Vinokur, *Phys. Rev. Lett.* **77**, 1596 (1996).  
<sup>16</sup>A. E. Koshelev and V. M. Vinokur, *Phys. Rev. B* **57**, 8026 (1998).  
<sup>17</sup>B. D. Biggs, M. N. Kumchur, J. J. Lin, S. J. Poon, T. R. Askew, R. B. Flippen, M. A. Subramanian, J. Gopalakrishnan, and A. W. Sleight, *Phys. Rev. B* **36**, 4021 (1987).  
<sup>18</sup>V. M. Vinokur, P. H. Kes, and A. E. Koshelev, *Physica C* **168**, 29 (1990).  
<sup>19</sup>G. Yang, P. Shang, S. D. Sutton, I. P. Jones, J. S. Abell, and C. E. Gough, *Phys. Rev. B* **48**, 4054 (1993).